Direct evidence and the mechanism of superheating in YBCO thin film

2004 J. Phys.: Condens. Matter 16 3819

(http://iopscience.iop.org/0953-8984/16/23/002)

INSTITUTE OF PHYSICS PUBLISHING JOURNAL OF PHYSICS: CONDENSED MATTER

J. Phys.: Condens. Matter **16** (2004) 3819–3826 PII: S0953-8984(04)76912-X

Direct evidence and the mechanism of superheating in YBCO thin film

X Yao[1,2,4], J Hu[1], T Izumi[3] and Y Shiohara[3]

[1] Department of Physics, Shanghai Jiao Tong University, 1954 Huashan Road, Shanghai 200030, People's Republic of China
[2] State Key Laboratory for Metal Matrix Composites, Shanghai Jiao Tong University, 1954 Huashan Road, Shanghai 200030, People's Republic of China
[3] Superconductivity Research Laboratory, 1-10-13 Shinonome Koto-ku, Tokyo 135-0062, Japan

E-mail: xyao@sjtu.edu.cn

Received 24 February 2004
Published 28 May 2004
Online at stacks.iop.org/JPhysCM/16/3819
DOI: 10.1088/0953-8984/16/23/002

Abstract

We report a novel-superheating phenomenon in $YBa_2Cu_3O_z$ (Y123) oxide films (over 45 K), which were prepared by vapour deposition on MgO substrates. The origin of this superheating could be mainly attributed to the positive change of surface energy in peritectic melting, during which Y123 melts into the Y_2BaCuO_5 (Y211) solid and the Ba–Cu–O liquid. It was found that the heterogeneous melting initiates at the Y123/MgO interface and the molten liquid does not wet MgO and Y123. These melting features of Y123 films explain the delaying of the melting process.

(Some figures in this article are in colour only in the electronic version)

1. Introduction

During a phase transition of melting, from a solid to a liquid, the change in value of surface free energy may have two possibilities: positive and negative. If it takes a positive value, the temperature of the phase transition is higher than the thermodynamic melting point (T_m) to gain a driving force for the formation of new phases, which is called a superheating. In most metals and their alloys, the melting generally does not require superheating because of two characteristics. Firstly, liquid metals wet the parent solid. Once the melting occurs, a complete liquid layer immediately covers the solid. Hence, the surface free energy change, $\Delta\gamma = \gamma_{SL} + \gamma_{LV} - \gamma_{SV} < 0$, is negative and no superheating is required, where γ_{SL}, γ_{LV} and γ_{SV} are interfacial energies between two phases of solid/liquid, liquid/vapour and

[4] Address for correspondence: Department of Physics, Shanghai Jiao Tong University, 1954 Huashan Road, Shanghai 200030, People's Republic of China.

solid/vapour, respectively. Secondly, the melting initiates around defect sites (e.g., solid–vapour free surfaces and internal grain boundaries) due to their high free energy [1], leading to melting at a temperature lower than T_m. For this reason, some low dimensional materials melt at temperatures much lower than their T_m values [2].

On the other hand, melting behaviour related to superheating has been reported for some specific cases. A crystallographic shape effect, leading to a superheating of 2–3 K, has been found for Pb triangular platelets bounded by the (111) surface [3], indicating a strong anisotropy of surface energy [4]. Further, the superheating of nanoparticles has been observed, when they are embedded in a high T_m matrix [4, 5], such as In and Ag embedded in Al and Ni, respectively. This superheating is related to a strong bonding from the high T_m matrix and a lack of free surface. Moreover, by means of rolling, a superheating of 6 K was reported to occur in a two-dimensional (2D) Pb thin film, which is sandwiched between Al layers [6]. To sum up, all the above-mentioned superheating phenomena are mainly associated with metallic materials and their melting behaviours, demonstrating a structure such as embedded particles or confined thin films. However, there remains some uncertainty about other superheating materials and structures.

In this paper, we report a novel superheating phenomenon in a $YBa_2Cu_3O_z$ (Y123 or YBCO) superconductor thin film. Unlike the previously reported superheating in metallic systems, the YBCO superheating phenomenon involves an oxide material with a peritectic melting, during which a Y_2BaCuO_5 (Y211) solid as well as a Ba–Cu–O liquid (BCO) is produced as the following peritectic reaction:

$$\text{Y123 (solid)} \rightarrow \text{Y211 (solid)} + \text{BCO (liquid)}.$$

Unlike a confined structure, this 2D thin film layer, prepared on the MgO substrate by vapour deposition, has one free surface and one semi-coherent interface. Acting as a seed-layer, these YBCO thin films were superheated up to 45 K and then were used for the liquid phase epitaxy (LPE) growth of REBCO superconductors, which have higher peritectic temperatures (T_p) than the YBCO oxide. In brief, this work extends our understanding of the superheating mechanism to different materials with different morphological features.

2. Experimental procedures

YBCO thin films were deposited on MgO single crystals by the pulsed laser deposition (PLD) technique and were then used as seed-crystals. These films are highly *c*-axis oriented and present a 0° relationship: $[100](001)_{YBCO} \parallel [100](001)_{MgO}$, with MgO substrates, examined by their XRD patterns and atomic force microscope (AFM) images. The Ba–Cu–O solvent was prepared by melting high quality $Ba_3Cu_4O_z$ powders. The Nd solute is supplied from the Nd_2O_3 crucible. NdBCO thick films were grown by the top-seeded solution-growth (TSSG) technique in air at about 1055 °C. The initial stage of LPE was studied by a vertically-dipping experiment as shown in figure 1, which was conducted with a continuous travelling mode at a rate of 1 mm s^{-1}.

In order to study the melting mechanism of YBCO thin films, a high temperature optical microscope (OLYMPUS BX51M with a heating stage LK 1500) was used for *in situ* observation of the melting of the YBCO thin film. The temperature calibration was conducted by using pure silver ribbons. Surface microstructures were characterized by Nomarski optical microscopy and atomic force microscopy (AFM). The compositional analysis was carried out by electron probe microscopic analysis (EPMA) to investigate the different phases and element distributions.

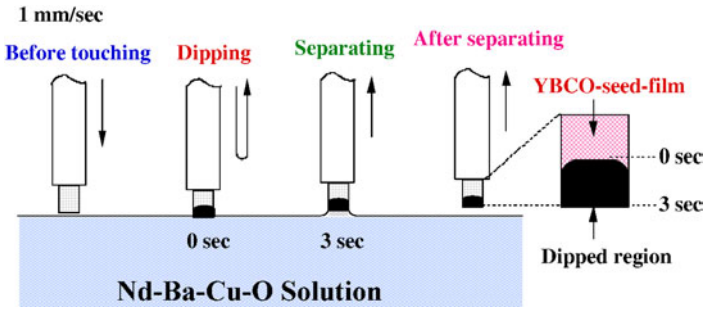

Figure 1. Schematic illustration of a vertically dipping experiment.

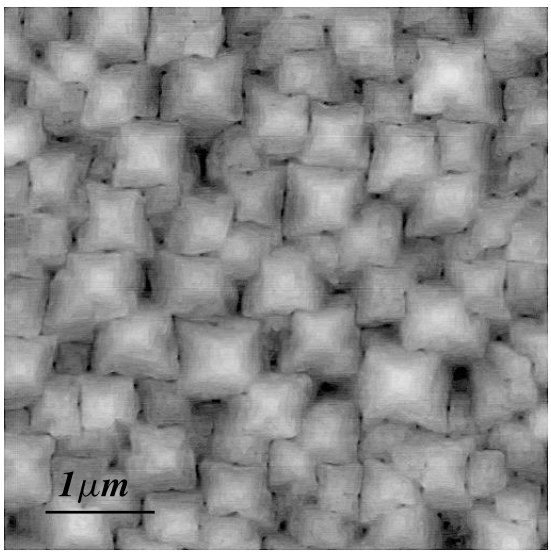

Figure 2. An AFM image showing a vapour-deposited YBCO seed-film structure.

3. Results and discussions

3.1. YBCO-seeded NdBCO LPE growth

With a predominant *c*-axis (and a few *a*-axis) oriented grains, the vapour-deposited YBCO films are characteristically polycrystalline and have an epitaxial orientation relationship of [100](001)YBCO ∥ [100](001)MgO as shown in the AFM image in figure 2. Using these YBCO ($T_p \sim 1010\,^{\circ}C$) thin-film seeds, the liquid phase epitaxy of the NdBCO thick film was successfully realized at a processing temperature of 1057 °C. After mechanical polishing, the AFM image displays a quasi-atomically smooth surface with a roughness of about 1 nm. The value of FWHM of the rocking curve at the (005) peak is 0.164°. All the above indicate that an NdBCO thick film has a high crystallinity although a hetero-seed of YBCO was used.

In order to study the mechanism of YBCO-seeded NdBCO growth (YSNG), a vertical-dipping experiment [8] was performed. Figure 3 is an optical micrograph of a vertically-dipped LPE specimen, showing a liquid-untouched region on the top side and a liquid-dipped region on the bottom side, which displays the microstructural development from the YBCO seed-film to the NdBCO epitaxy thick film. When the specimen was pulled down into the liquid, the YBCO

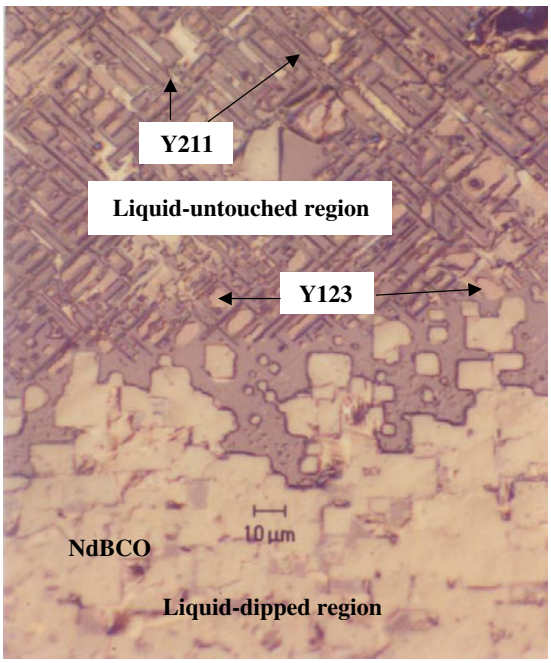

Figure 3. An optical micrograph showing microstructures of a vertically-dipped specimen from the liquid-untouched region on the top side to the liquid-dipped region on the bottom side.

grains underwent heating from room temperature to 1057 °C, which is higher than the T_p of YBCO, and became thermodynamically unstable. Consequently, we can observe Y_2BaCuO_5 (Y211) grains and solidified Ba–Cu–O (BCO) liquid in the liquid-untouched region, which are the result of the YBCO decomposition. Needle-shaped Y211 grains are well aligned on the MgO, covered with the BCO liquid. The most important feature in figure 3 is that undecomposed YBCO particles are clearly observed in the liquid-untouched region, implying a superheating phenomenon since they endured a high processing temperature above T_p of YBCO. The orientation relationship between YBCO on the undipped region and NdBCO grains on the dipped region can be confirmed. Firstly, NdBCO grains exhibit a square morphology and 0°-orientation [8] on the MgO substrate as shown in figure 3, indicating that the NdBCO grain has an epitaxial orientation relationship of [100](001)NdBCO ∥ [100](001)MgO. This behaves similarly to the YBCO seed-grain on MgO. Secondly, EPMA mapping was used to determine the Nd and Y distribution near the dipping boundary. It was found that there are yttrium-segregated regions close to the boundary in the dipped side, which are visible only and exactly underneath the initially-grown NdBCO grains as displayed in figure 4. Altogether it verifies an epitaxial relationship of [100](001)YBCO ∥ [100](001)NdBCO and a superheating phenomenon of the YBCO thin film, i.e., the YBCO seed is responsible for the formation of NdBCO grains.

Unlike the normal melting from a solid to a liquid, the products of peritectic melting include the Y211 solid and the BCO liquid. Therefore, the change of surface free energy can be expressed by

$$\Delta\gamma = \gamma_{Y211/Y123} + \gamma_{Y211/V} + \gamma_{Y123/L} + \gamma_{V/L} - \gamma_{Y123/V} \tag{1}$$

where $\gamma_{Y211/Y123}$, $\gamma_{Y211/V}$, $\gamma_{Y123/L}$, $\gamma_{V/L}$, and $\gamma_{Y123/V}$ represent interfacial energies between two phases (Y211/Y123, Y211/vapour, Y123/liquid, vapour/liquid and Y123/vapour). The

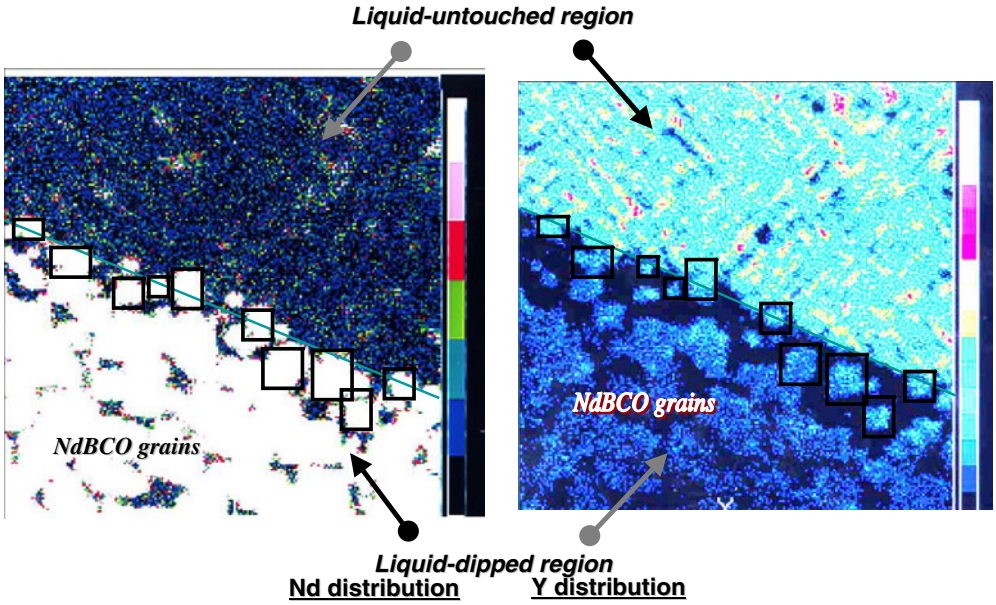

Figure 4. EPMA mapping images showing Nd and Y distributions at the boundary between the undipped region on the top side and the dipped region on the bottom side.

existence of superheating in the YBCO film indicates that the non-wetting condition is obeyed, i.e., $\Delta\gamma > 0$. This positive change in the surface energy could be interpreted by the formation of Y211 solid, which requires a driving force of superheating for balance. In addition, the interface of MgO/Y123 has a semi-coherent relationship between $[100]_{Y123}$ and $[100]_{MgO}$ ($\sim$9%); the melting temperature of MgO is about 2800 °C, which is much higher than that of YBCO. Therefore YBCO has a strong bonding with MgO at the interface, leading to suppression of YBCO melting. Moreover, the solid phase of Y211 has a different composition and structure from the low temperature phase of Y123. Thus the formation of the new phase involves an atomic migration and a crystal structure change. In contrast, when a metallic material melts it experiences a lattice change from a long-range order solid into a short-range order liquid, which involves a simple rigidity catastrophe [7] of crystal lattice without an atomic migration. In brief, taking both thermodynamic and kinetic considerations, the Y123 peritectic melting is reasonably expected to require superheating.

3.2. In situ observation of the melting process of YBCO thin film

The superheating of the YBCO-coated MgO substrate was further studied by *in situ* observations using a high temperature optical microscope. With a heating rate of 5 K min^{-1}, heating to its peritectic temperature of 1010 °C and holding for 3 min, the YBCO thin film remained almost unchanged [9]. Figure 5 shows optical micrographs of vapour-deposited YBCO thin films, demonstrating the microstructural evolution of the Y123 decomposition. When the thin film was superheated up to 1030 °C, the Y211 phases appeared initially as a dashed line, indicating a primary stage of the Y123 decomposition. These Y211 phases then gradually emerged as a solid straight line with increasing temperature (at temperatures of 1035 and 1042 °C). These observations indicate that the Y123 melting initiates at the interface between the MgO substrate and the Y123 film. Taking heterogeneous nucleation in Y123

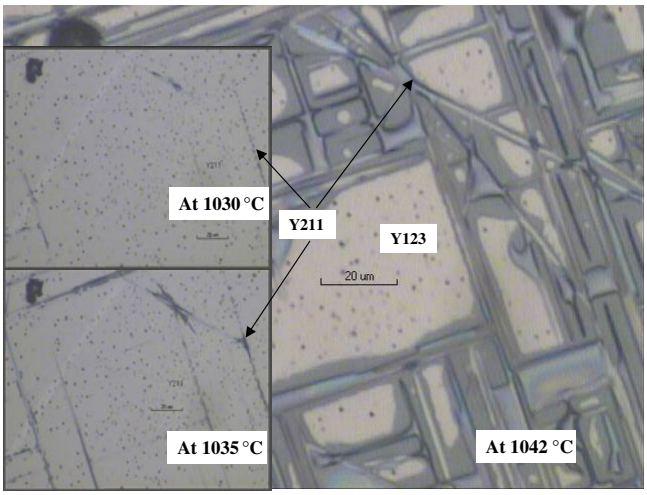

Figure 5. Optical micrographs showing the evolution of the Y211 nucleation from the interface of MgO/YBCO.

melting into consideration, there are three possible defect sites in the vapour-deposited YBCO thin films: the free surface of the Y123 thin film, the grain boundary of Y123, and the interface of MgO/Y123. On the other hand, from the Y211 crystallization point of view, the nucleation and growth of the Y211 solid phase should create a low energy interface. By XRD analysis, needle-shaped Y211 grains with a *c*-axis in a long direction [9] are detected, which are well aligned on the MgO substrate and present an epitaxial relationship of $[001]_{Y211} \parallel [110]_{MgO}$. The misfit of $[001]_{Y211}/[110]_{MgO}$ and $[010]_{Y211}/[110]_{MgO}$ is 5.26% and 2.81%, respectively. In contrast, the misfit of $[001]_{Y211}/[110]_{Y123}$ and $[010]_{Y211}/[110]_{Y123}$ are 2.88% and 9.74%, respectively. It is clear that the (100) plane of Y211 has a lower lattice mismatch with the MgO substrate than with the Y123 phase. Moreover, Y211 favourably forms a Y211/MgO interface with a high thermal stability due to the high melting temperature of MgO, while the Y211 phase cannot nucleate on the Y123 surface during the YBCO melting. Finally, in comparison with the YBCO polycrystalline structure, as a nucleation site of Y211, MgO is preferable for its single crystallinity and atomically flat surface. In brief, the origins of the preferential YBCO melting or Y211 nucleation at the interface can be interpreted by a strong bond at the interface of MgO/Y211 because of its low surface energy and high thermal stability.

Figure 6 presents an optical micrograph from real-time observation of YBCO melting at a temperature of 1043 °C. A large drop of BCO liquid, as marked, appears at the front of a marked Y123 grain, as a consequence of the Y123 decomposition. It was found that this BCO liquid rolled away immediately from the melting interface of the Y123 grain and swept across the MgO surface to Y211 needles as shown on the upper right-hand side of figure 6, which was taken after 10 s holding. This result suggests that the BCO liquid wets neither the parent phase of Y123 nor the MgO substrate, i.e., $\gamma_{Y123/L} > \gamma_{Y123/V}$, and $\gamma_{MgO/L} > \gamma_{MgO/V}$. Generally, the melting continues as long as a driving force exists (even if it is very small). However, the nucleation of melting requires a sufficiently large driving force. Since liquid keeps moving away from the solid and cannot facilitate the growth of the Y123 melting, a continuous driving force for nucleation of melting is required. On the other hand, a locally low temperature region was induced owing to the endothermic reaction of Y123 melting. All the above-mentioned points cause the delay of melting. In comparison with the melting mode in metallic systems,

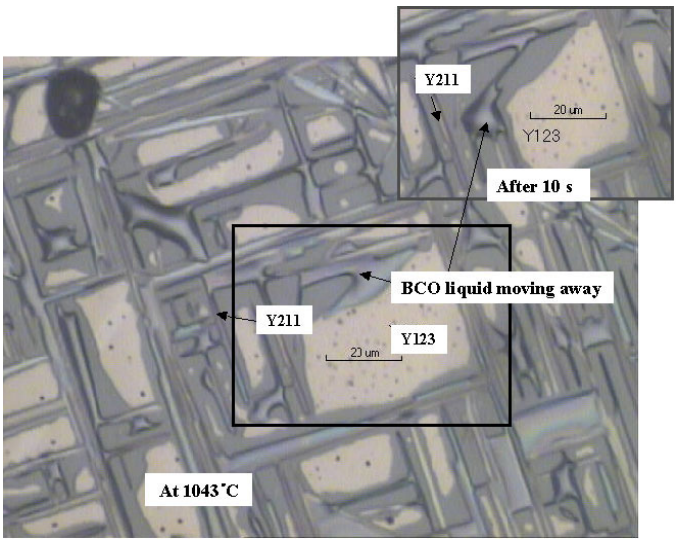

Figure 6. Optical micrographs displaying the liquid movement from the Y123 melting front to the Y211 phase.

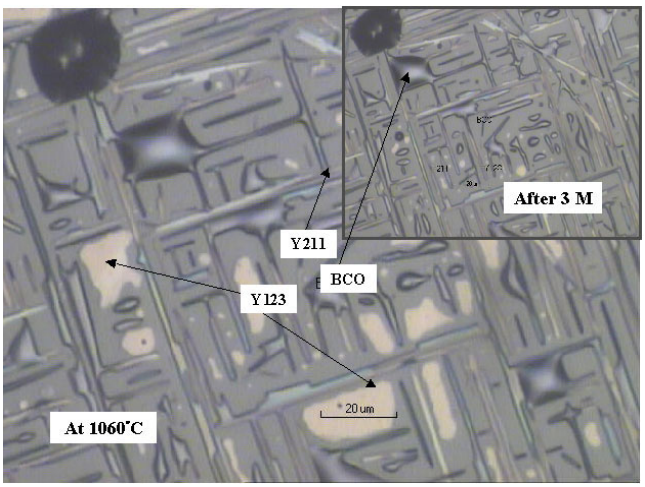

Figure 7. Optical micrographs show superheated vapour-deposited thin film at temperatures up to 1060 °C.

it is found that once a liquid layer forms on the surface it moves at a substantial rate into the solid [10]. In those systems, because a solid surface is wetted by its own melt, the surface induced melting leads to melting occurring at a temperature lower than T_m [11]. In contrast, the melting of YBCO thin film is delayed up to 1060 °C, as shown in figure 7. The superheating at this temperature can be maintained for at least 3 min, as shown on the upper right-hand side of figure 7, in which there are fewer Y123 grains.

4. Conclusions

In conclusion, a novel-superheating phenomenon was found in a vapour-deposited $YBa_2Cu_3O_z$ (YBCO) thin film, a non-metallic system. This oxide melting is distinctively characterized by

(1) a positive surface energy change due to the formation of a solid and a liquid via the YBCO peritectic melting;
(2) a low energy interface of the YBCO/MgO substrate because of semi-coherent bonding; and
(3) a liquid migration from the melting front caused by the non-wetting of Ba–Cu–O liquid with both YBCO and MgO.

Acknowledgments

Xin Yao is grateful to Professor D G McCartney for careful English correction and for financial support from Cheung Kong Scholars Program (CKSP), the National Science Foundation of China (grant no 50272038), the National High Technology Research & Development Program of China (grant no 2002AA306261), and the Ministry of Education (grant no 20030248010 and K0293003). A part of this work was carried out while Xin Yao worked at the Superconductivity Research Laboratory (ISTEC/SRL) in Japan.

References

[1] Cahn R W 1986 *Nature* **323** 491
[2] Buffat Ph and Borel J P 1976 *Phys. Rev.* A **13** 2287
[3] Herman J W and Elsayed-Ali H E 1992 *Phys. Rev. Lett.* **69** 1228
[4] Chattophdhyay K and Goswami R 1997 *Prog. Mater. Sci.* **42** 287
[5] Lu K and Jin Z H 2001 *Curr. Opin. Solid State Mater. Sci.* **5** 39
[6] Zhang L, Jin Z H, Zhang L H, Sui M L and Lu K 2000 *Phys. Rev. Lett.* **85** 1484
[7] Tallon J L 1989 *Nature* **342** 658
[8] Nomura K, Hoshi S, Yao X, Nakamura Y, Izumi T and Shiohara Y 2001 *J. Mater. Res.* **16** 979
[9] Hu J, Yao X and Rao Q L 2003 *J. Phys.: Condens. Matter* **15** 7149
[10] Couchman P R and Jesser W A 1977 *Nature* **269** 481
[11] Müller P and Kern R 2003 *Surf. Sci.* **529** 59